Cr stable isotope fractionation by evaporation from silicate melts

Klemme S[1,*], Genske F[1], Sossi PA[2], Berndt J[1], Renggli CJ[1], Stracke A[1]

[1] Institut für Mineralogie, Universität Münster, Corrensstrasse 24, 48149 Münster, Germany
[2] ETH Zürich, Department of Earth Sciences, Sonneggstrasse 5, 8092 Zürich, Switzerland
[*] corresponding author

Abstract

We present new experimental results of Cr isotope fractionation during degassing of silicate melts. Our experiments at oxidizing conditions (in air) at 1 bar total pressure show that evaporative loss of Cr is substantial and depends on run duration and on temperature (between 1350 and 1500 °C). The stable Cr (δ^{53}Cr) isotope compositions of the evaporation residues were analyzed by thermal ionization mass spectrometry using the double spike method. Our results indicate that during degassing the lighter isotope ^{52}Cr is enriched in the gas phase and consequently the residual melt becomes enriched in the heavier ^{53}Cr isotope in a mass-dependent fashion. The kinetic isotopic fractionation factor, α, derived from our experimental data is 0.9995±0.0001, which is significantly different from the fractionation factor predicted for an ideal gas composed of CrO_3, α_{kin} = 0.995. Our experimentally-determined value of α is consistent with diffusive transport of CrO_3 (g) away from the melt surface, proportional to the inverse cube-root of the reduced masses of the two isotopologues. We hypothesize that Cr loss by evaporation may be recorded by Cr isotopes in terrestrial magmas with sufficiently high oxygen fugacities erupting near the surface, which are plausibly found in lava lakes or erupting arc magmas.

1. Introduction

Loss of volatile elements due to evaporation from silicate magmas on Earth and other planetary bodies is a common process, which leads to the observed elemental fractionation of volatile elements in volcanic systems (Menard et al., 2014; Moune et al., 2006; Renggli and Klemme, 2020; Rubin, 1997; Stefansson et al., 2017). Whilst the loss of volatile elements during degassing of magmas has been studied recently (Norris and Wood, 2017; Sossi et al., 2019), relatively few experimental studies investigated the consequence of evaporation on the isotopic composition of the melt or the evaporating gas phase (Badro et al., 2021; Mendybaev et al., 2021; Neuman et al., 2022; Ni et al., 2021; Nielsen et al., 2021; Richter et al., 2009; Richter et al., 2007; Sossi et al., 2020; Wimpenny et al., 2019, Renggli et al. 2022).
If a volatile element has more than one stable isotope, the stable isotopes of this element are susceptible to fractionation during evaporation as described

by the kinetic theory of gases. Recent studies show convincingly that the observed isotopic fractionation of Zn, Cl and other (moderately) volatile elements in lunar rocks were due to evaporation (e.g., Boyce et al., 2018; Day and Moynier, 2014; Dhaliwal et al., 2018; Sossi et al., 2018). However, the locus and extent of such evaporation is debated owing to the lack of independent constraints on the magnitude of isotopic fractionation produced during evaporation of these elements from silicate melts. In order to enable the quantitative interpretation of stable isotopic compositions of igneous rocks, new experimental data are of crucial importance.

Here we set out to investigate the behavior of Cr and its stable isotopes (^{50}Cr, ^{52}Cr, ^{53}Cr, and ^{54}Cr) during degassing of silicate melts. Chromium is a geochemically refractory minor element in the Earth's mantle and in peridotite it is mainly hosted by garnet, spinel, and pyroxenes (e.g., Fumagalli and Klemme, 2015; Klemme, 2004, Ziberna and Klemme, 2016). During partial melting of the mantle Cr, has a bulk partition coefficient of about 1 (Liang and Elthon, 1990) and hence terrestrial komatiites contain several thousand µg/g Cr, but basalts typically contain lower amounts due to Cr retention in chromite (e.g., Roeder and Reynolds, 1991). However, in a cosmochemical context Cr is also moderately volatile (Sossi and Fegley, 2018; Sossi et al., 2019; Wijbrans et al., 2015), and evaporation from silicate melts can be significant, especially under oxidizing conditions owing to the stability of oxygen-bearing gas species (Sossi et al., 2019).

To model mass dependent kinetic isotope fractionation during evaporation from a silicate magma with a finite quantity of the element of interest, the Rayleigh distillation equation is commonly employed, and a critical component of these is the kinetic fractionation factor, α. As fractionation factors for many volatile elements have not been measured experimentally, the so-called theoretical values for α are commonly employed (e.g., Dhaliwal et al., 2018). These theoretical values are based on the kinetic theory of gases, which states that $^{i/j}\alpha$ is equal to $(m_j/m_i)^{0.5}$, where m denotes the molar masses of isotopes *i* and *j*. However, several recent studies on the kinetic isotope fractionation of K (Richter et al., 2011; Wang and Jacobsen, 2016; Yu et al., 2003) and Mg (Davis et al., 2015; Richter et al., 2009; Richter et al., 2007) showed that the experimentally determined values of α diverge from theoretical estimates, and that the latter are theoretical maximum values on the extent of fractionation. In detail, the $(m_j/m_i)^{0.5}$ dependence is expected to apply only in the specific end-member case of an ideal gas in which the mean free path is large, which occurs under near-vacuum conditions. To understand natural degassing processes on Earth, Sossi et al. (2020) developed a theoretical formalism based on experimental results of Cu and Zn evaporation at 1 bar, and showed that the fractionation factor depends on the mechanism by which the evaporating species is released from the surface. For a near-stationary gas (i.e., one where its advective velocity, *v*, approaches 0), these authors deduced that binary diffusion of the gas species through the

atmosphere was the rate-limiting step, resulting in a dependence of α on the ratio of diffusion rates of the two isotopes, *i* and *j*, through a gas of molar mass *k*, where $\alpha = (D_{ik}/D_{jk})^{2/3}$, or, at constant temperature and pressure, $(\mu_{jk}/\mu_{ik})^{1/3}$, where μ is the reduced mass, $m_i m_k/(m_i+m_k)$.

Previous experiments (e.g., Norris and Wood, 2017; Sossi et al., 2019) showed that Cr is moderately volatile and that elemental loss from silicate melts was significant, especially under oxidizing conditions. Furthermore, recent geochemical studies showed that lunar basaltic rocks are significantly lighter in their Cr isotopic composition ($\delta Cr^{53/52}$) than terrestrial basalts (Bonnand et al., 2016; Sossi et al., 2018). Sossi et al. (2018) argue that the observed isotopic fractionation of lunar basalts may be caused by a large scale evaporation event where Cr partitioned into an oxidized gas species namely $CrO_2(g)$. This interpretation only holds if the fractionation occurred under equilibrium conditions rather than being kinetically driven, as the force constant for $CrO_2(g)$ is higher than that for Cr^{3+} or Cr^{2+} dissolved in the silicate melt. Kinetic fractionation would be excluded, as it always results in an enrichment of the heavy isotope in the residue during evaporation. In contrast, Bonnand et al. (2016) interpreted the lunar Cr isotopic data by the crystallization of Cr-spinel from a lunar basaltic magma, while Shen et al. (2020) suggest it may arise during partial melting. As there is no experimentally determined data on the fractionation of stable Cr isotopes during degassing of melts, the apparent paradox could not be resolved. However, recent experimental work on the calibration of fractionation factors between Cr-spinel and silicate melt as a function of fO_2 indicate that the melt has lower δCr^{53} than spinel (Bonnand et al., 2020), albeit to smaller extents as oxygen fugacities approach those of the reducing conditions that typify lunar mare basalt genesis (e.g., IW-2.5 to IW+0.2; Fogel et al. 1995).

In summary, all of the above arguments highlight the need for experimentally determined isotopic fractionation factors, both for isotopic fractionation during evaporation and for mineral precipitation from melts. To progress on resolving these matters, we set out to experimentally investigate the isotopic fractionation of Cr during evaporation from a silicate melt at oxidizing conditions.

2. Experimental and analytical techniques

2.1. Starting materials

Starting materials were synthesized from reagent grade oxides (SiO_2, Al_2O_3, MgO) and $CaCO_3$. The MgO starting material was fired at 1,000°C for 2 h, and subsequently stored at 110°C. The bulk composition of the starting material corresponds to the composition of the anorthite-diopside eutectic. Five grams of this starting material were weighed out and mixed in an agate mortar under acetone to obtain a homogeneous mixture. A nominal amount of

5000 µg/g Cr was added to the starting material using a 10,000 mg/l ICP-MS (in 5% HNO_3) plasma standard solution (Merck KGaA, Germany) and mixed with the starting material again in an agate mortar. The resulting mixture was de-carbonated and denitrified in a Pt crucible at 1000°C for 2 h. The final starting material mixture was then vitrified at 1400°C for 5 min, and most of the resulting glass was reground in an agate mortar. Electron microprobe analysis of several chips of the starting material glass showed that the glass was homogenous with the following composition (wt.%): CaO 24.1, MgO 10.6, Al_2O_3 15.2, and SiO_2 50.1, identical to the composition of the anorthite-diopside eutectic. An aliquot of the starting material was dissolved in concentrated HF-HNO_3 and analyzed with TIMS (see details below) and the analysis showed that the starting material contains about 4,500 µg/g Cr (Table 1).

2.2. Experiments

Experiments were performed using the Pt-wire loop technique (e.g., Beyer et al., 2013; Borisov, 2001; Wijbrans et al., 2015). To prepare the loops, we mixed about 20 mg of starting material powder with a synthetic organic glue into a highly viscous slurry, and we loaded this mixture onto a 0.1 mm-thick Pt-wire loop. The samples were then introduced into the hotspot of a vertical alumina tube furnace (Gero GmbH, Germany). Temperature was controlled with a thermocouple external to the alumina tube by a Eurotherm (Schneider Electric, Germany) controller, limiting fluctuations to within 1 °C. Temperatures were independently measured with a Type B thermocouple, and adjusted as necessary (Klemme and O'Neill, 1997). All experiments were run in air.

Run duration is reported from the time of sample insertion and therefore includes a several minute-long thermal equilibration time (Sossi et al., 2019). Charges were quenched by dropping them into a beaker with distilled water. Table 1 lists all experimental run conditions, together with the isotopic compositions and Cr concentrations.

2.3. Analytical methods

2.3.1. Major and trace elements

The major element composition of the starting material was measured with a JEOL JXA 8530F Electron Microprobe. The microprobe was calibrated with a variety of pure oxides and minerals of known chemical composition. To test for trace element homogeneity of the run products, we analyzed (see Fig 1) the Cr concentrations of a test run with laser ablation inductively coupled mass spectrometry (LA-ICPMS) at the University of Münster. For this, the glass bead was cut through the center with a low-speed diamond wheel saw,

it was mounted in epoxy resin and the mount was subsequently polished using a series of diamond pastes. Details of the LA-ICPMS method have been reported elsewhere (e.g., Wijbrans et al., 2015).

2.3.2. Cr isotope measurements

We analyzed partially degassed residual quenched melt samples for their isotopic composition using the double spike technique with thermal ionization mass spectrometry (TIMS) at the University of Münster, Germany.

All acids used during the chemical procedures were double-distilled from analytical grade reagents (ROTH®) in individual Savillex DST-1000 stills. Each sample was weighed and dissolved with concentrated HF and HNO_3 (4:1) in a TFE Parr bomb at 180 °C for 5 days to ensure complete digestion. After cooling and drying down at 120 °C the samples were repeatedly dissolved and treated with HCl at 110 °C to decompose fluorides. Note, that sample sizes of the glass beads were typically between 5 and 20 mg and fluorides were easily decomposed by addition of 6 N HCl. The temperature of 110 °C for drying down was chosen to avoid the potential partial loss of Cr, and hence isotope fractionation, during evaporation of chromyl chloride (CrO_2Cl_2), which has a boiling point of 117 °C.

Appropriate amounts of a 10 µ/g ^{50}Cr (abundance of 0.57315) -^{54}Cr (abundance of 0.39030) double-spike solution, i.e. aiming at an optimized sample-Cr (µg) to spike-Cr (µ) ratio of 0.3 (after Rudge et al. (2009)), were added to the clear sample solutions and equilibrated at 120 °C overnight prior to Cr purification via chromatography. We added the double spike solution to fully dissolved samples to avoid potential loss of unknown spike fractions if the spike solution had been added to the coarsely crushed sample beads. Immersing a 6 N HCl spike solution in a 6 N HCl sample solution enhances equilibration. The chosen and calibrated ^{50}Cr-^{54}Cr double spike allows a large range for optimal spiking, that is minimized errors are achieved with a double spike proportion in the double spike-sample mix between 0.1 and 0.6; calibrations and error calculations were performed using the double spike toolbox by Rudge et al. (2009). Subsequent chemical separation followed protocols that are detailed elsewhere (e.g., Bonnand et al., 2016; Bonnand et al., 2017; Schoenberg et al., 2016; Trinquier et al., 2008). Briefly, separation followed a three-column purification scheme, starting with the removal of Fe by anion chromatography, before Cr was purified using two cation columns (e.g., Trinquier et al., 2008; Yamakawa et al., 2009).

Pure Cr solutions were measured on a thermal ionization mass spectrometer (ThermoScientifc Triton TIMS) at the Institut für Mineralogie, University Münster. About 1 µg of Cr was dissolved in 6 N HCl and loaded on previously outgassed Re filaments in a sandwich of an activator solution, which contains silica gel, boric acid and Al. The sample was dried down slowly on the filament and the current was increased until the sample turned a dull red color. This resulted in homogenous pale green glass deposits on the

filament. Typical Cr runs consisted of 160 to 180 cycles, with 8.4 s of integration per cycle, which were collected once the signal reached an intensity of 4-6 V on ^{52}Cr, with slowly increasing ion beams. The reproducibility of the method was assessed by multiple processing of a spiked NIST SRM 979 solution, which gave $\delta^{53}Cr = 0.01 \pm 0.06$ ‰ (2 S.D, n = 5).

Rock standards processed along with the samples yielded $\delta^{53}Cr$ values of -0.19 ± 0.02 ‰ (2 S.D, n = 4) for JB-1, and -0.10 ± 0.09 ‰ (2 S.D, n = 5) for BHVO-2, which are in good agreement with compiled literature values (JB-2 with $\delta^{53}Cr = -0.18 \pm 0.05$ ‰, BHVO-2 with $\delta^{53}Cr = -0.13 \pm 0.05$ ‰ (Bauer et al., 2018; Cole et al., 2016; Gueguen et al., 2016; Liu et al., 2019; Schoenberg et al., 2016; Zhu et al., 2018). Internal measurement errors (2 S.E.) were typically between 0.02 and 0.08 ‰ on $\delta^{53}Cr$. Results of Cr isotope compositions and Cr contents of the experimental samples and reference materials are reported in Table 1.

3. Discussion / Results

3.1. Experimental and analytical results

The isotopic compositions of the staring material, the degassed residual glasses, along with the experimental run conditions, are listed in Table 1.

Table 1 Starting material composition, experimental run conditions, and analytical results

sample no.	t / min	T / °C	Cr conc / µg/g	$\delta^{53}Cr$	2SD
SKM-Cr1			4,464 (220)	-0.09	0.03
SKECr-2	70	1,505	417(21)	1.07	0.09
SKECr-3	120	1,505	151(17)	1.81	0.15
SKECr-33	15	1,505	3,697(210)	0.10	0.03
SKECr-35	25	1,505	1,444(79)	0.51	0.03
SKECr-37	45	1,505	944(45)	0.79	0.04
SKECr-25	60	1,457	2,044(41)	0.2	0.20
SKECr-27	140	1,457	165(21)	1.4	0.1
SKECr-28	120	1,360	1,833(90)	0.12	0.02
BHVO-2			293(8)	-0.10	0.09
JB-1			457(11)	-0.19	0.02

SKM-Cr1 refers to the starting material mixture. The SKE sample no. are run numbers. t / min = run duration in minutes, T / °C = run temperature in °C, Cr conc = Cr concentrations in residual glasses in µg/g, the uncertainties are given in brackets. The Cr isotopic data are reported as $\delta^{53}Cr$, the per mille deviation of the $^{53}Cr/^{52}Cr$ ratio of the sample from the NIST SRM 979 standard, together with its associated 2SD (2 x standard deviation) uncertainty. See analytical techniques for details.

3.2. Homogeneity of residual glasses

The *in-situ* analyses across the residual glass samples show that they are, within the analytical uncertainties, homogeneous from core to rim, despite

having lost up to ~99.3 % of their initial Cr budget (Fig. 1). If the degassing process would have been much faster than the diffusive transport of an element within the melt, evaporation should have caused Cr depletion in the boundary layer of the residual melt. That this is not observed (Fig. 1) indicates that the characteristic timescale of degassing is much greater in our runs than the diffusion rates of Cr within the melt (see Sossi et al. (2019)) for a detailed discussion on these matters). The lack of zoning thus indicates that diffusion in the liquid was not the rate-limiting factor that controlled the measured element abundances and isotopic compositions of the residual glasses (Richter et al., 2011). To estimate a minimum value for the diffusion coefficient, D_{Cr} (likely to be entirely trivalent under the conditions studied, e.g. (Berry et al., 2006)), we employed a finite difference model in spherical co-ordinates with a changing boundary condition dictated by the evaporation rate (Sossi et al. 2020). Given the ratio between the Cr concentration in the degassed melt and the undegassed starting material (X_{Cr}^{t}/X_{Cr}^{0}) is 0.0067 (Fig. 1), we compute that, in order for the difference in concentration between core and rim (r = 1.2 mm) not to exceed 10 % relative (the approximate uncertainty of the LA-ICP-MS analyses), a $\log(D_{Cr})$ of >-8.5 is required, where D is in m^2/s. This is more than two orders of magnitude faster than measured for Cr tracer diffusion in high-alumina andesitic melt at 1,400 °C (Koepke and Behrens, 2001). Insofar as liquids with more depolymerised structures (e.g., basalts) promote faster tracer diffusion than do polymerised liquids (e.g., rhyolites) and that diffusion is thermally activated (e.g. Lowry et al. 1982), these results are consistent with the lower SiO_2 and Al_2O_3 contents (50.1 wt. % *vs.* 61.8 wt. % and 15.2 wt. % vs. 19.5 wt. %, respectively) and higher temperatures (1,500 °C vs. 1,400 °C) examined herein.

Fig. 1 Homogeneity of residual glasses

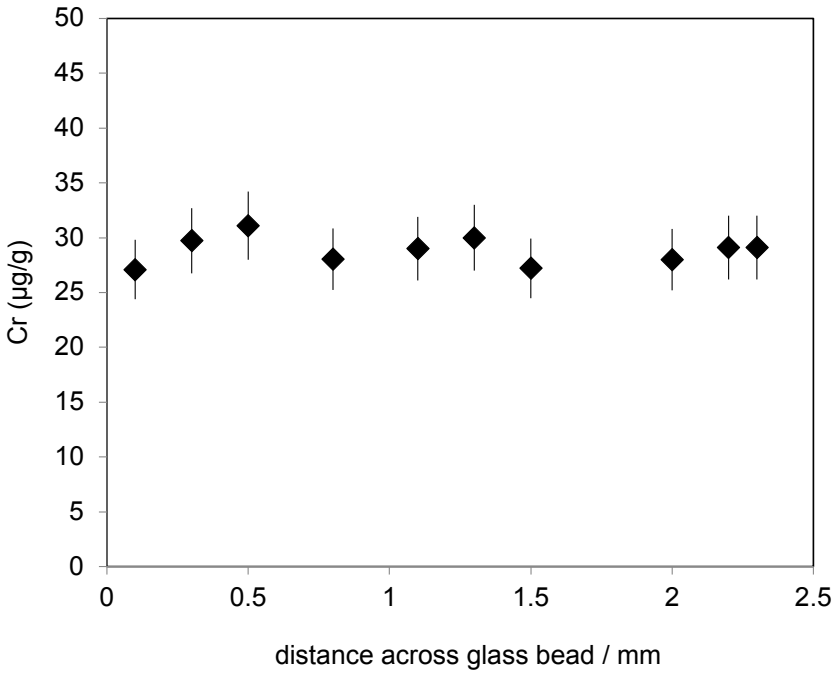

Fig. 1. Cr concentration profile of a test run product, i.e. a residual glass bead (1,500°C, 200 min, air). The run was done under identical run conditions as the runs presented in Table 1.

3.3. Fractionation of the stable isotopes of Cr during evaporation from a silicate melt

Before discussing our experimental results, we briefly consider the theoretical isotope fractionation between ^{52}Cr and ^{53}Cr. Using the relation for ideal kinetic isotopic fractionation for evaporation into a vacuum

$$^{i/j}\alpha_{kin} = \sqrt{\frac{m_j}{m_i}} \qquad \text{eq. (1)}$$

where m_j and m_i are the masses of the light and heavy isotopologue, respectively. Therefore, the theoretical maximum isotopic fraction factor for Cr, should it exist as Cr^0 (i.e., the monatomic gas), is 0.990. If, however, Cr degassing involves electron transfer, i.e., a redox reaction (Sossi et al., 2019) resulting in the stability of CrO (g), CrO_2 (g) or CrO_3 (g), then the theoretical maximum isotopic fractionation depends on the species of Cr in the gas phase. Using equation (1), this would result in α_{kin} values of 0.993, 0.994 and 0.995, respectively.

When plotting the Cr isotopic composition of the residual glasses against the Cr concentration (Fig 2) it is obvious that the heavy ^{53}Cr is enriched relative to

^{52}Cr in residual glasses, and that there is an inverse relationship between Cr concentration and isotopic composition of the residues. Furthermore, our data shows that significant (or analytically resolvable) Cr isotopic fractionation only occurs only after about 50% of the initial budget of Cr is lost due to degassing.

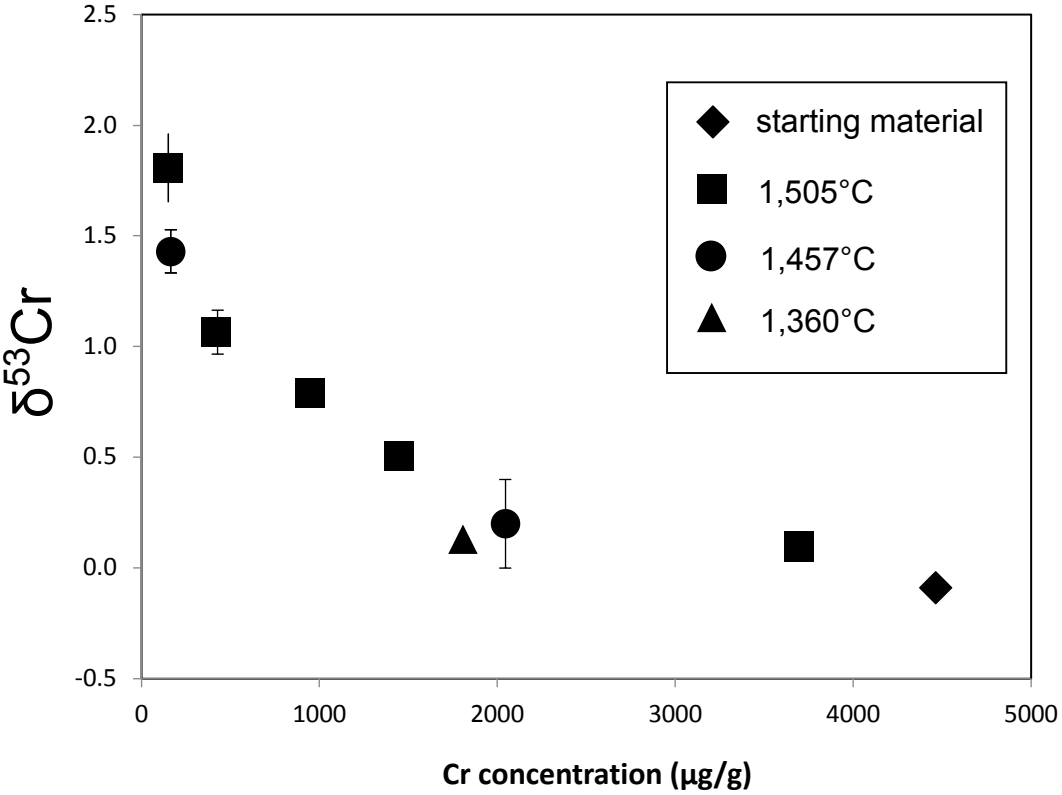

Fig. 2: Cr isotopic composition of residual glasses (δ^{53}Cr) plotted against their Cr concentration (µg/g). Diamond: starting material composition. Error bars plotted when larger than symbols.

Figure 3 depicts the experimentally determined Cr isotopic composition of all our degassed residual glasses plotted against their Cr fraction remaining relative to the starting material (X_{Cr}^{t} / X_{Cr}^{0}) = *f*. . When stable isotope data are plotted in this way, the isotopic compositions that were fractionated by a Rayleigh fractionation will fall on a line with a slope equal to 1000 (1- α_{kin}) where α_{kin} is the kinetic isotope fractionation between the gas phase and the residual melt. The kinetic isotope fractionation factor is hence independent of the composition of the condensed phase. Figure 3 (all data fitted) depicts all of our data in this way resulting in α_{kin} = 0.9995±0.0001.

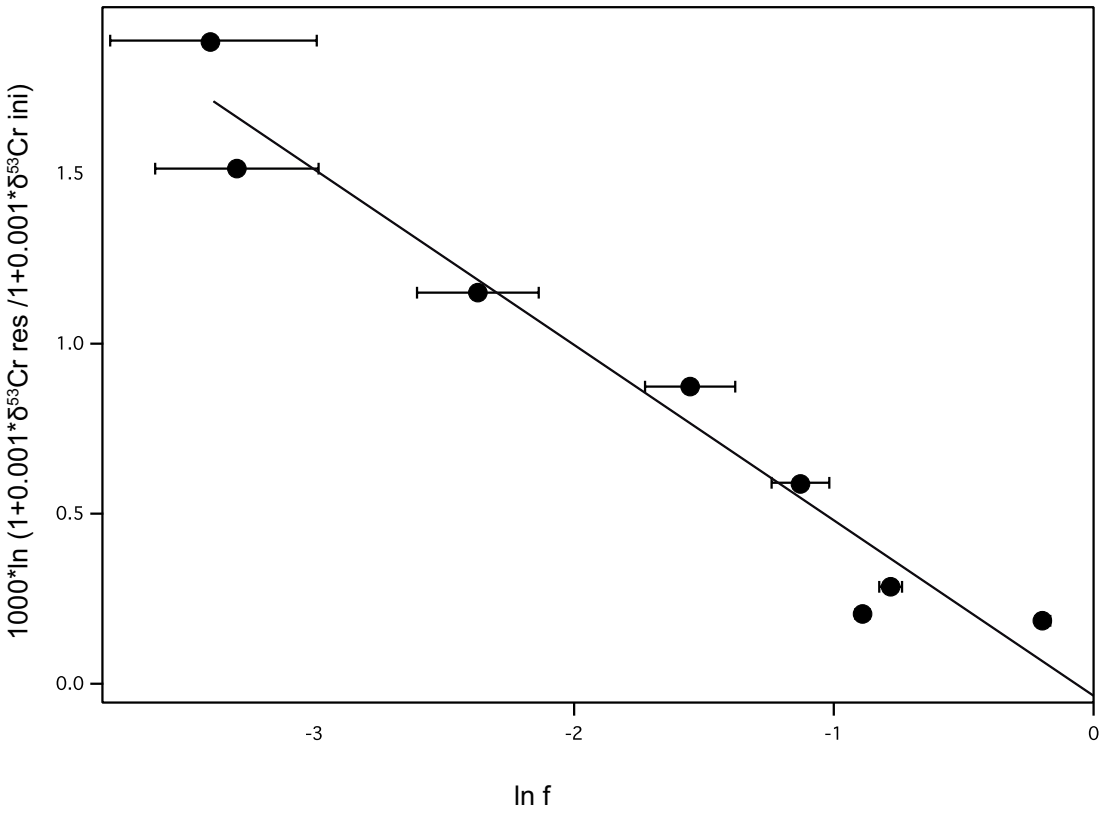

Fig. 3: Cr isotopic composition of the partially degassed residual glasses listed in Table 1 plotted as 1000*ln (1+0.001* $\delta^{53}Cr_{res}$ /1+0.001* $\delta^{53}Cr_{ini}$) versus ln f, where ln f is the fraction of ^{52}Cr remaining in the residual glass and $\delta^{53}Cr_{res}$=($^{53}Cr/^{52}Cr$) of the residual glasses, and $\delta^{53}Cr_{ini}$ = ($^{53}Cr/^{52}Cr$) of the undegassed starting material).

4. Discussion

The main motivation of this study was to experimentally determine Cr isotopic fractionation factors that may be used to interpret Cr isotope variations in terrestrial basalts and other igneous rocks.

Our data clearly shows that Cr isotopes are strongly fractionated during degassing of a silicate melt under oxidizing conditions (Fig. 2). Degassing enriches the lighter isotope ^{52}Cr in the gas phase and consequently, the residual melt becomes enriched in the heavier ^{53}Cr isotope in a mass-dependent fashion. The kinetic isotopic fractionation factor, α, derived from our experimental data is 0.9995±0.0001 (Fig. 3), which is much higher (i.e., the isotopic difference between gas and melt is smaller) than than predicted from the kinetic isotope fractionation factor α_{kin} (eq. 1). For evaporation in air, the thermodynamically-stable Cr gas species is CrO_3, leading to α of 0.995, lower than that observed in our runs.

Sossi et al. (2020) developed a theory to describe isotopic fractionation during evaporation, which states that, in environments at 1 bar where the gas surrounding the evaporating sample is stationary or slow moving, diffusion of the element through the gas controls transport away from the surface. From

empirical correlations of mass transport rates with dimensionless numbers, it can be shown that the mass transport coefficient is proportional to $D_{ik}^{2/3}$ (the Chilton-Colburn equation where D stands for the binary diffusion coefficient (Liu and Bautista, 1981; Sossi et al., 2020). Therefore, the fractionation of two isotopes is proportional to $(D_{ik}/D_{jk})^{2/3}$. For binary diffusion, that is, the diffusion of one component, *i*, through a gas of a second component, *k*, which is given by the Chapman-Enskog equation (Chapman and Cowling, 1990), D is proportional to $\mu^{-1/2}$, where μ is the reduced mass. As such, the fractionation factor at the diffusive limit is equal to $(\mu_{jk}/\mu_{ik})^{1/3}$. Substituting in the masses of of $^{53}CrO_3$ and $^{52}CrO_3$, *i* = 101 g/mol and *j* = 100 g/mol and that of the surrounding gas medium, air, for which *k* = 28.8 g/mol, results in $^{53/52}\alpha Cr_{vap\text{-}liq}$ = 0.9993. This figure, within uncertainty, matches that derived from our experiments (0.9995±0.0001), and strongly supports that CrO_3 (g) is the predominant gas species during evaporation from silicate melts (e.g., Sossi et al. (2019)) in air *a posteriori*.

We hypothesize that Cr loss by evaporation may be recorded by Cr isotopes in terrestrial magmas with sufficiently high oxygen fugacities erupting near the surface, which are plausibly found in lava lakes or erupting arc magmas. In the next section we will explore possible scenarios under which such fractionation may occur.

4.1. Cr isotope fractionation in magmatic systems

4.1.1. Komatiites

We first consider several recent studies on the Cr isotopic signatures of komatiites (Jerram et al., 2020; Sossi et al., 2016; Wagner et al., 2021). Komatiites were erupted at very high temperatures (T>1,400°C, e.g., Green, 1975; Nisbet et al., 1993) with a low viscosity (e.g., Huppert et al., 1984), and consequently komatiites may show Cr isotope fractionation due to evaporative Cr loss. Even though some komatiites, notably from the Barberton Greenstone Belt show textural evidence for having erupted subaqueously (Dann, 2001), it remains possible that others were subaerial in origin, and thus may have undergone direct degassing upon exposure to the atmosphere.

Of the komatiite samples studied by Jerram et al. (2020), the most isotopically fractionated example in the Belingwe flows (Zn14) is from the A3 zone, about 4 m beneath the top of the flow facies. The chilled margin of the flow (TN-01), which may be expected to have the heaviest composition should degassing have occurred, has a Cr isotope composition similar to that of the upper mantle (~-0.14 ‰). Variation in $\delta^{53}Cr$ among komatiite suites, both within flow and between different localities, is of the same order as the analytical precision (Jerram et al., 2020; Sossi et al., 2018; Wagner et al., 2021). It is likely that komatiite flows do not show any isotopic fractionation due to degassing because many were erupted subaqueously (Flament et al., 2008) and the high temperature difference (ΔT) between the water and/or country

rocks into which they were emplaced produced chilled margins, meaning degassing was not sustained over time. Indeed, Huppert et al. (1984) considered that for quenching in seawater, a margin of not more than a few centimeters would form on timescales much shorter than that for the emplacement of the flow. These chill zones efficiently acted as a carapace to prevent any outgassing from the komatiite surface, and allowing them to cool and crystallize relatively slowly in their interiors. That no isotopic fractionation is observed in samples from the chilled margins suggests that they cooled sufficiently rapidly and/or at sufficiently reducing conditions (~FMQ; (Nicklas et al., 2018)) to prevent significant Cr outgassing, given that the proportion of Cr remaining in the melt scales with exp(-t) (Tsuchiyama et al., 1981) and the partial pressure of CrO_3 (g) with $fO_2^{3/4}$ (Sossi et al., 2019). In support of this notion, Cr contents of komatiite chilled margins are remarkably homogeneous (~2500 ppm; Sossi et al. 2016), and similar to those of the Earth's mantle (Liang and Elthon, 1990; Palme and O'Neill, 2014). Consequently, it seems likely that komatiites were likely emplaced rapidly from depth owing to their low viscosities (e.g., Huppert et al. (1984))

4.1.2. Subaerial degassing from magmas

Chromium degassing and concurrent isotope fractionation may also occur during subaerial volcanic eruptions. Thermodynamic models for the speciation of Cr in vapors produced from volcanic fumaroles, such as at Kudryavy volcano, indicate the stability of several species, the most important of which at high temperatures (>827°C) is $Cr^{4+}O_2H_2$ (Churakov et al., 2000), although $CrCl_2$ and CrO_2Cl_2 are present in about equal proportions at oxygen fugacities just above the fayalite-magnetite-quartz buffer. A similar tendency is observed for other Group VI metals (W and Mo), in which the hydrolyzed or chlorinated forms of their stable oxides (MoO_4H_2, WO_4H_2 and MoO_2Cl_2, WO_2Cl_2) may occur (Churakov et al., 2000; Wahrenberger et al., 2002). To better understand the speciation of Cr in volcanic vapours, we calculated the speciation of Cr in the gas phase in the system Cr-Cl-C-O by Gibbs free energy minimization (e.g. see Renggli et al. (2017) for more details on the method). The speciation at 1,200°C and 1bar is shown in Figure 4 as a function of the oxygen fugacity. In Cl-rich systems (Cl/Cr=2) appropriate for arc related volcanic systems, the dominant Cr gas species are CrO_2Cl and CrO_2Cl_2 at oxidizing conditions, and $CrCl_2$ at reducing conditions (Fig.4 a). However, in Cl-poor systems the speciation changes from CrO_3 at oxidizing conditions (above $\log fO_2 \approx -3$; or FMQ+5.5), to CrO_2Cl, CrO_2 and Cr, with decreasing $\log fO_2$ (Fig.4 b). Since lava lakes degas into air (at $\log fO_2 = -0.68$) we only consider the species CrO_3 to model the effect of degassing on the Cr isotope composition.

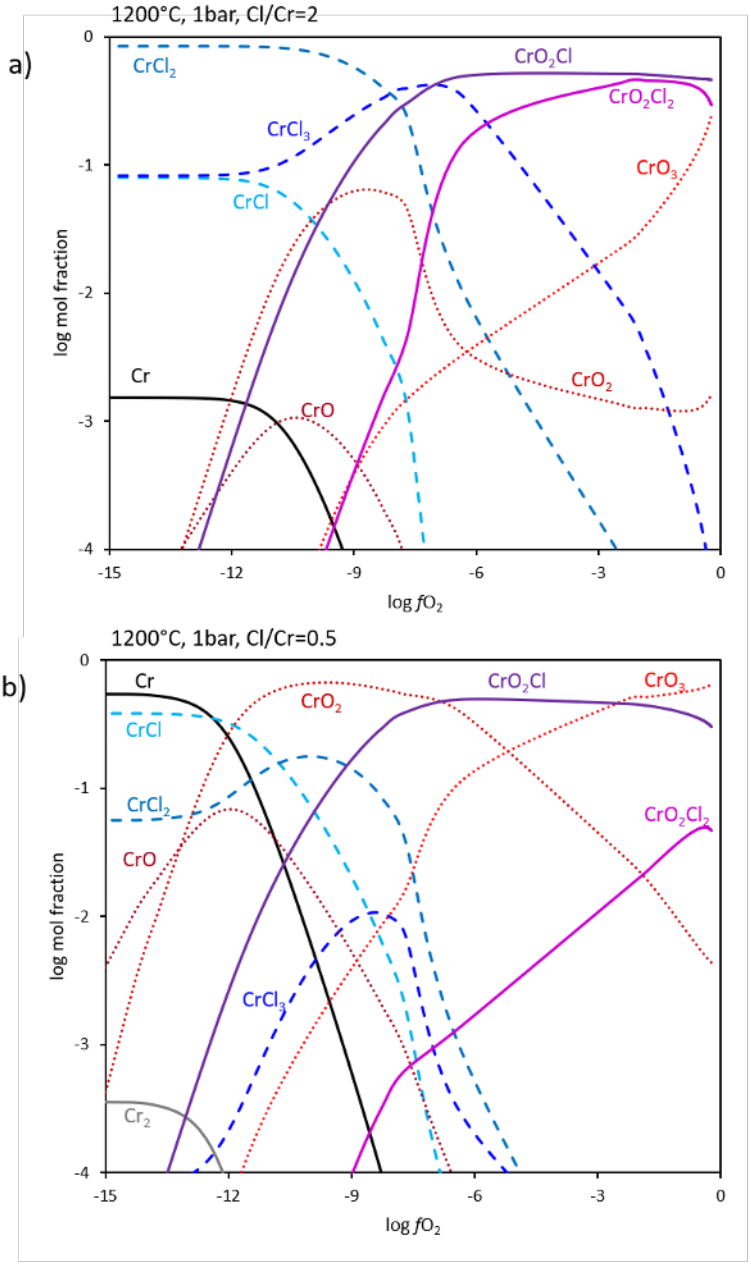

Fig. 4: Chromium gas speciation in the Cr-Cl-C-O system calculated by Gibbs free energy minimization with the software package HSC Chemistry (2018). We included the following Cr-bearing gas species in the calculation: Cr, Cr_2, CrO, CrO_2, CrO_3, CrCl, $CrCl_2$, $CrCl_3$, $CrCl_4$, CrO_2Cl, and CrO_2Cl_2. The log mol fractions of the gas species are shown as a function of logfO_2 at 1,200°C and 1bar. We varied the molar Cl/Cr ratio in the two calculations: a) Cl/Cr = 2; b) Cl/Cr = 0.5. At low Cl abundances in air (logfO_2 = -0.68) CrO_3 is the main Cr-bearing gas species. The Fayalite-Magnetite-Quartz (FMQ) buffer lies at log fO_2 = -8.4 at 1200 °C (O'Neill, 1987)

However, for assessing whether the Cr isotope composition of the outgassed species differs from that of the magma from which they are exsolved requires understanding of their volatility, as well as the physical conditions under which degassing occurred. An empirical assessment of the relative volatilities of the elements during eruption can be determined from elemental enrichment factors, EF, defined as (e.g., Aiuppa et al. (2003)):

$$EF(x) = \frac{(x/Al)_{gas}}{(x/Al)_{magma}}$$

Where *x* refers to the abundance of an element x, and Al (chosen here) is an element taken to be nominally refractory. A recent compilation of EFs for Cr in both arc volcanoes and rift/hotspot volcanoes by Zelenski et al. (2021) indicates a relatively high volatility for Cr, with a $\log(K_D^{gas\text{-}melt})$ of -1.42±1.32 in arc volcanoes and -3.17±1.43 in rift/hotspot volcanoes. These K_D values correspond to log(EF) of 2.90 and 1.15, respectively, according to the Yb-normalization used by Zelenski et al. (2021). These data highlight two important characteristics; i) Cr is moderately volatile during volcanic eruptions and ii) it is more volatile during arc volcanic eruptions than in dry, intraplate magmatic activity. This latter point may be in part related to the elevated oxygen fugacities of arc magmas relative to their intraplate counterparts, a variable that may favours the vaporisation of Cr (Sossi et al., 2019). Thus we expect that significant Cr isotope fractionation occurs in the gas phase that is formed during volcanic degassing.

As many volcanic gases carry large amounts of Cr (e.g., with a Cr-flux in the gas phase of 3-25 kg day^{-1} (Mather et al., 2012) at Kilauea Volcano, Hawaii, USA) we expect that precipitates from the gas phase or rocks that contain a thin veneer of such precipitates are charaterzied by a lighter Cr isotope signature than the magma. However, to our knowledge, Cr isotopes in rocks from such geological settings have not been analyzed, yet. Furthermore, a recent paper (Yobo et al., 2022) links light Cr isotopes (together with data on $^{187}Os/^{188}Os$, $^{87}Sr/^{86}Sr$) in marine sediments to large volcanic eruptions in the Caribbean (Turgeon and Creaser, 2008) and to an extensive ocean anoxic event (OAE 2) that occurred around 95 million years ago. We suggest that the observed isotopic fractionation may have been caused by degassing but further data on these matters are clearly needed.

4.1.3. Degassing of Cr from a lava lake

In the final paragraph we evaluate if Cr degassing from a silicate magma lake may cause Cr isotope fractionation. The Kilauea Iki lava lake (Hawaii, USA) is basaltic, with a roughly cylindrical form and with a radius and a height of ~400 m (Fig. 5A). The cooling front progressed from the surface to its interior over a timespan of ~30 years from the initial eruption 1959 to the time when the last drill cores were taken in 1988 (e.g., Helz et al. (1994)).

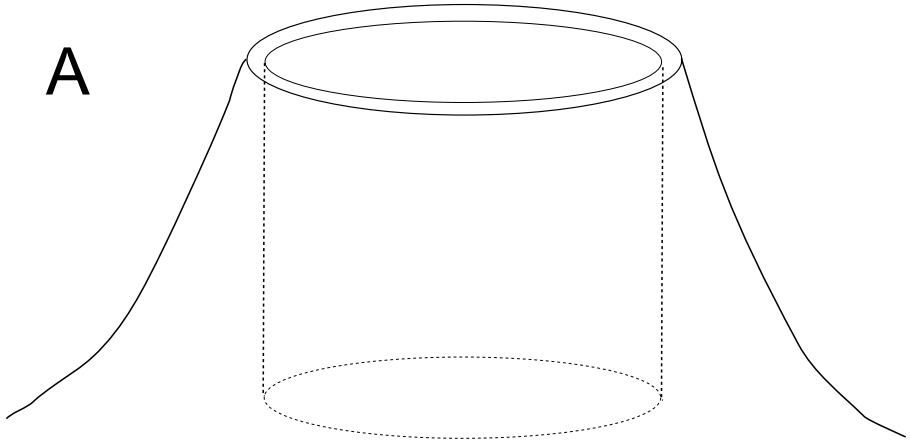
A

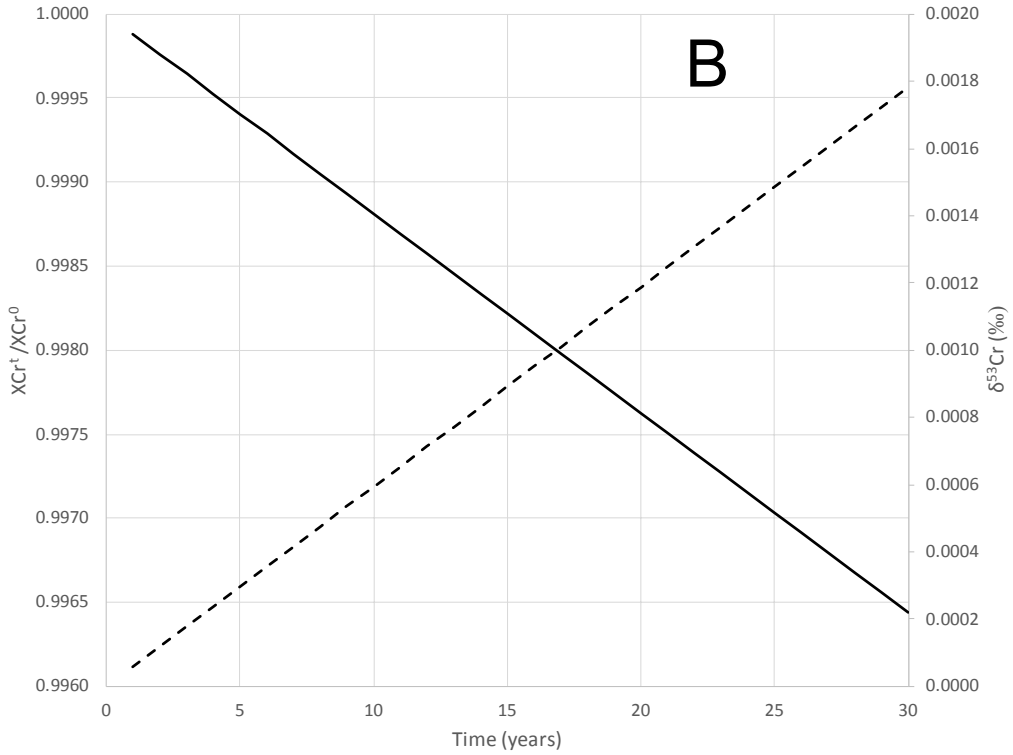
B
1.0000
0.9995
0.9990
0.9985
0.9980
0.9975
0.9970
0.9965
0.9960
XCr^t /XCr^0
0.0020
0.0018
0.0016
0.0014
0.0012
0.0010
0.0008
0.0006
0.0004
0.0002
0.0000
δ^{53}Cr (‰)
0
5
10
15
20
25
30
Time (years)

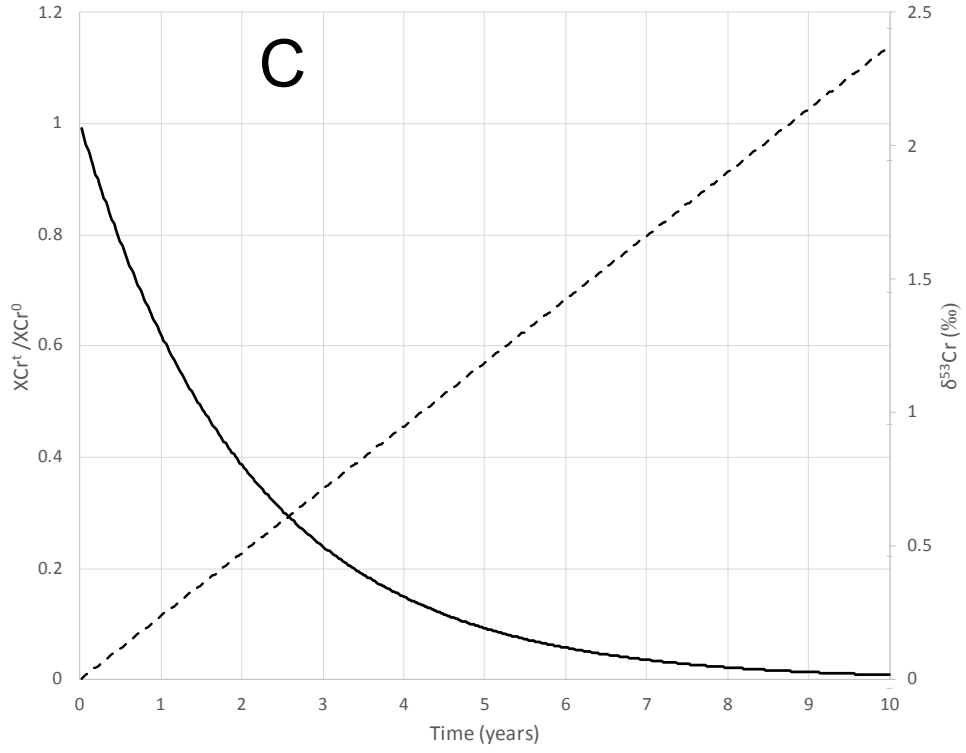
C
1.2
1
0.8
0.6
0.4
0.2
0
XCr^t /XCr^0
2.5
2
1.5
1
0.5
0
δ^{53}Cr (‰)
0
1
2
3
4
5
6
7
8
9
10
Time (years)

520

Fig. 5: A: Schematic diagram of a lava lake with 400 m diameter and 400 m depth. See text for discussion. **B:** Calculated Cr loss and Cr isotope fractionation from the lava lake depicted in A. The solid line shows the calculated amount of Cr that is lost due to evaporation from a convecting lava lake (400 m diameter and 400 m deep). XCr^t = Cr lost due to evaporation after time *t*, XCr^0 = initial Cr concentration of the lava. The dashed line shows the corresponding $\delta^{53}Cr$ calculated using our new isotope fractionation factors and a recently published general degassing model (Sossi et al. 2019). Our data shows that even after 30 years only a very small amount of Cr has degassed and consequently the isotopic composition of the residual melt has only very slightly changed. **C:** The solid line (as in A) shows the calculated Cr evaporative loss and the dashed line depicts the calculated $\delta^{53}Cr$ of a residual 0.1 m deep layer of melt on top of the lava lake (see text for details). If such a thin layer of melt degasses, Cr is rapidly lost but a 40% loss of Cr takes about one year of steady degassing and this amount of evaporation would correspond to an increase of $\delta^{53}Cr$ of about 1.2‰.

To calculate the vaporization rate of CrO_3 (g) from the surface of the lake, we modified the equation of Sossi et al. (2019), originally devised for vaporization from a sphere, to that from the top surface of a cylinder to approximate the lava lake. As such, the geometric term '3/r' in eq. 8 (and its derivatives) of Sossi et al. (2019), becomes 1/2h, where h is the height of the region undergoing vaporization. In the model, we examined the simplified case of a basaltic liquid evaporating at a constant temperature (T_0 = 1,400°C) in 1 bar of air (fO_2 = 0.21 bar). The oxidation state of Cr is presumed therefore to be entirely trivalent, leading to the reaction:

$$CrO_{1.5}\ (l)\ +\ \frac{3}{4}\ O_2(g)\ =\ CrO_3(g)$$

Where the partial pressure of CrO_3 is given:

$$p(CrO_3)\ =\ K.a(CrO_{1.5}).f(O_2)^{3/4}$$

We assume an activity coefficient, $\gamma CrO_{1.5}$ of 5 (Pretorius and Muan, 1992) while thermodynamic Gibbs Free Energies of O_2 (g), CrO_3(g) and Cr_2O_3(l) and are taken from the JANAF tables (Chase, 1998). For the nominal case of a 400 m deep lava lake, which is homogenized by convection, only 0.4 % of the total Cr budget can degas over its 30 year lifespan. Using our experimentally-determined fractionation factor, $^{53/52}Cr\ \alpha_{vap\text{-}liq}$ = 0.9995, this amounts to a $\delta^{53}Cr$ of the magma of 0.002 ‰, about an order of magnitude smaller than that currently detectable by modern analytical methods.

By contrast, if we assume a hypothetical 0.1 m - thick boundary layer on the surface, also at a constant temperature of 1,400 °C, then 99 % of the Cr budget can degas after 10 years, producing a total isotopic fractionation of $\delta^{53}Cr$ = +2.38 ‰. However, this extreme scenario is probably unrealistic as i) the magma is convecting such that mass transport delivers new batches of melt to the surface, and ii) an isolated surface boundary layer cools on the timescale of minutes. Even for a total degassing time of 1 day, a 0.1 m thick layer loses only 0.15 % of its Cr budget. We therefore consider that the most likely sites of Cr isotope fractionation occur during volcanic outgassing and/or

fire-fountaining, in which small beads of silicate liquid experience volatile loss over short timescales prior to cooling.

Summary

- New experiments on Cr degassing from silicate melts in a 1 bar gas-mixing furnace show that evaporative loss of Cr under oxidizing conditions (air) is substantial and the associated degree of Cr isotope fractionation varies in a predictable manner with run duration and temperature
- During degassing ^{52}Cr is enriched in the gas phase and the residual melt becomes enriched in the heavier ^{53}Cr isotope. The kinetic isotope fractionation factor, α, derived from the experiments is 0.9995±0.0001, significantly different from the so-called "theroretical" value $\alpha_{kin} = 0.995$.
- Evaporative Cr losses that can significantly affect the Cr content and the isotopic composition of the residual magma require very high temperatures and oxygen fugacities, as well as sustained heating to ensure extended loss timescales.
- Strongly degassed lavas or precipitates from a volcanic gas phase may show significant isotope fractionation of Cr and similarly-behaving volatile elements (i.e., W, Mo) during degassing of silicate melts under oxidizing conditions.

Keywords

Experimental petrology, stable isotope fractionation, Chromium isotopes, degassing, evaporation, fractionation factor

Acknowledgements

We are indebted to M. Trogisch for his sterling job in the sample preparation labs at Münster University, and to B. Schmitte for her expertly assistance with the electron microprobe and LA-ICP-MS measurements. Our thanks also go to P. Weitkamp, C. Fritzsche, S. Flunkert, A. Hardes, and L. Peuker for their help with the maintenance of the experimental laboratories. This study was partially supported by the Deutsche Forschungsgemeinschaft (DFG – Project-ID 263649064) and this is SFB TRR-170 publication No. 169. PAS thanks the Swiss National Science Foundation (SNSF) under Ambizione Fellowship No. 180025.

References

Aiuppa, A., Dongarra, G., Valenza, M., 2003. Degassing of trace volatile metals during the 2001 eruption of Etna Volcanism and the Earth's Atmosphere Geophysical Monograph. . American Geophysical Union, Washington, D.C., pp. 41-54.

Badro, J. et al., 2021. Experimental investigation of elemental and isotopic evaporation processes by laser heating in an aerodynamic levitation furnace. Comptes Rend Geosci., 353(1): 101-114.

Bauer, K.W. et al., 2018. Chromium isotope fractionation in ferruginous sediments. Geochim. Cosmochim. Acta, 223: 198-215.

Berry, A.J., O'Neill, H.S.C., Scott, D.R., Foran, G.J., Shelley, J.M.G., 2006. The effect of composition on Cr2+/Cr3+ in silicate melts. Am. Mineral., 91(11-12): 1901-1908.

Beyer, C., Berndt, J., Tappe, S., Klemme, S., 2013. Trace element partitioning between perovskite and kimberlite to carbonatite melt: New experimental constraints. Chem. Geol., 353: 132-139.

Bonnand, P. et al., 2020. The influence of igneous processes on the chromium isotopic compositions of Ocean Island basalts. Earth Planet. Sci. Lett., 532: 116028.

Bonnand, P., Parkinson, I.J., Anand, M., 2016. Mass dependent fractionation of stable chromium isotopes in mare basalts: Implications for the formation and the differentiation of the Moon. Geochim. Cosmochim. Acta, 175: 208-221.

Bonnand, P., Williams, H.M., Parkinson, I.J., Wood, B.J., Halliday, A.N., 2017. Corrigendum to “Stable chromium isotopic composition of meteorites and metal–silicate experiments: Implications for fractionation during core formation” [Earth Planet. Sci. Lett. 435 (2016) 14–21]. Earth Planet. Sci. Lett., 460: 315-316.

Borisov, A., 2001. Loop technique: dynamics of metal/melt equilibration. Mineral. Petrol., 71(1-2): 87-94.

Boyce, J.W. et al., 2018. Early loss, fractionation, and redistribution of chlorine in the Moon as revealed by the low-Ti lunar mare basalt suite. Earth Planet. Sci. Lett., 500: 205-214.

Chapman, S., Cowling, T.G., 1990. The mathematical theory of non-uniform gases. Cambridge University Press, Cambridge, UK, 422 pp.

Chase, M.W., 1998. NIST-JANAF thermochemical tables (Vol. 9, pp. 1-1951). Washington, DC: American Chemical Society.

Churakov, S.V., Tkachenko, S.I., Korzhinskii, M.A., Bocharnikov, R.E., Shmulovich, K.I., 2000. Evolution of composition of high-temperature fumarolic gases from Kudryavy volcano, Iturup, Kuril Islands: the thermodynamic modeling. Geochem. Int., 38(5): 436-451.

Cole, D.B. et al., 2016. A shale-hosted Cr isotope record of low atmospheric oxygen during the Proterozoic. Geology, 44(7): 555-558.

Dann, J.C. 2001. Vesicular komatiites, 3.5-Ga Komati Formation, Barberton Greenstone Belt, South Africa: inflation of submarine lavas and origin of spinifex zones. Bull. Volcan. 63, 462-481

Davis, A.M. et al., 2015. Isotopic mass fractionation laws for magnesium and their effects on Al-26-Mg-26 systematics in solar system materials. Geochim. Cosmochim. Acta, 158: 245-261.

Day, J.M.D., Moynier, F., 2014. Evaporative fractionation of volatile stable isotopes and their bearing on the origin of the Moon. Phil. Trans Roy. Soc.- Math. Phys. Sci., 372(2024).

Dhaliwal, J.K., Day, J.M.D., Moynier, F., 2018. Volatile element loss during planetary magma ocean phases. Icarus, 300: 249-260.

Flament, N., Coltice, N., Rey, P.F., 2008. A case for late-Archaean continental emergence from thermal evolution models and hypsometry. Earth Planet. Sci. Lett., 275(3-4): 326-336.

Fumagalli, P., Klemme, S., 2015. Mineralogy of the Earth: Phase Transitions and Mineralogy of the Upper Mantle. In: Schubert, G. (Ed.), Treatise on Geophysics. Elsevier, Amsterdam, pp. 7-31.

Green, D.H., 1975. Genesis of archean peridotitic magmas and constraints on archean geothermal gradients and tectonics. Geology, 3: 15–18.

Gueguen, B. et al., 2016. The chromium isotope composition of reducing and oxic marine sediments. Geochim. Cosmochim. Acta, 184: 1-19.
Helz, R.T., Kirschenbaum, H.K., Marinenko, J.W., Qian, R., 1994. Whole-rock analyses of core samples from the 1967, 1975, 1979 and 1981 drillings of Kilauea Iki lava lake, Hawaii 94-684, US Geological Survey.
Huppert, H.E., Sparks, R.S.J., Turner, J.S., Arndt, N.T., 1984. Emplacement and cooling of komatiite lavas. Nature, 309(5963): 19-22.
Jerram, M. et al., 2020. The δCr53 isotope composition of komatiite flows and implications for the composition of the bulk silicate Earth. Chem. Geol., 551: 119761.
Klemme, S., 2004. The influence of Cr on the garnet-spinel transition in the Earth's mantle: experiments in the system MgO-Cr2O3-SiO2 and thermodynamic modelling. Lithos, 77(1-4): 639-646.
Klemme, S., O'Neill, H.S.C., 1997. The reaction MgCr2O4+SiO2=Cr2O3+MgSiO3 and the free energy of formation of magnesiochromite (MgCr2O4). Contrib. Mineral. Petrol., 130(1): 59-65.
Koepke, J., Behrens, H., 2001. Trace element diffusion in andesitic melts: An application of synchrotron X-ray fluorescence analysis. Geochim. Cosmochim. Acta, 65(9): 1481-1498.
Liang, Y., Elthon, D., 1990. Evidence from chromium abundances in mantle rocks for extraction of picrite and komatiite melts. Nature, 343(6258): 551-553.
Liu, C.Y. et al., 2019. High-Precision Measurement of Stable Cr Isotopes in Geological Reference Materials by a Double-Spike TIMS Method. Geostand. Geoanalyt. Res., 43(4): 647-661.
Liu, T.K., Bautista, R.G., 1981. Prediction of the chromium-oxide oxidation rate from the equilibrium-constants and the mass-transfer coefficients at high-temperatures. Oxid. Met., 15(3-4): 277-286.
Lowry, R.K., Henderson, P., Nolan, J. (1982). Tracer diffusion of some alkali, alkaline-earth and transition element ions in a basaltic and an andesitic melt, and the implications concerning melt structure. Contrib. Mineral. Petrol., 80(3): 254-261.
Mather, T.A. et al., 2012. Halogens and trace metal emissions from the ongoing 2008 summit eruption of Kilauea volcano, Hawaii. Geochim. Cosmochim. Acta, 83: 292-323.
Menard, G. et al., 2014. Gas and aerosol emissions from Lascar volcano (Northern Chile): Insights into the origin of gases and their links with the volcanic activity. J. Volcan. Geotherm. Res., 287: 51-67.
Mendybaev, R.A. et al., 2021. Experiments quantifying elemental and isotopic fractionations during evaporation of CAI-like melts in low-pressure hydrogen and in vacuum: Constraints on thermal processing of CAIs in the protoplanetary disk. Geochim. Cosmochim. Acta, 292: 557-576.
Moune, S., Gauthier, P.J., Gislason, S.R., Sigmarsson, G., 2006. Trace element degassing and enrichment in the eruptive plume of the 2000 eruption of Hekla volcano, Iceland. Geochim. Cosmochim. Acta, 70(2): 461-479.
Neuman, M. et al., 2022. High temperature evaporation and isotopic fractionation of K and Cu. Geochim. Cosmochim. Acta, 316: 1-20.
Ni, P., Macris, C.A., Darling, E.A., Shahar, A., 2021. Evaporation-induced copper isotope fractionation: Insights from laser levitation experiments. Geochim. Cosmochim. Acta, 298: 131-148.
Nicklas, R.W., Puchtel, I.S., Ash, R.D., 2018. Redox state of the Archean mantle: Evidence from V partitioning in 3.5-2.4 Ga komatiites. Geochim. Cosmochim. Acta, 222: 447-466.
Nielsen, S.G. et al., 2021. Thallium isotope fractionation during magma degassing: evidence from experiments and Kamchatka arc lavas. Geochem. Geophys. Geosys., 22(5): e2020GC009608.
Nisbet, E.G., Cheadle, M.J., Arndt, N.T., Bickle, M.J., 1993. Constraining the potential temperature of the Archean mantle—a review of the evidence from komatiites. Lithos, 30: 291–307.
Norris, C.A., Wood, B.J., 2017. Earth's volatile contents established by melting and vaporization. Nature, 549(7673): 507-510.

O'Neill, H.S.C., 1987, Quartz-fayalite-iron and quartz-fayalite-magnetite equilibria and the free energy of formation of fayalite (Fe2SiO4) and magnetite (Fe3O4). Am. Mineral., 72: 67-75

Palme, H., O'Neill, H.S.C., 2014. Cosmochemical Estimates of Mantle Composition. In: Holland, H.D., Turekian, K.K. (Eds.), Treatise on Geochemistry. Elsevier, Amsterdam, Netherlands, pp. 1-39.

Pretorius, E. B., Muan, A., 1992. Activity–composition relations of chromium oxide in silicate melts at 1500 C under strongly reducing conditions. J. Am. Ceramc Soc., *75*(6): 1364-137.

Renggli, C.J., King, P.L., Henley, R.W., Norman, M.D., 2017. Volcanic gas composition, metal dispersion and deposition during explosive volcanic eruptions on the Moon. Geochim. Cosmochim. Acta, 206: 296-311.

Renggli, C.J., Klemme, S., 2020. Experimental constraints on metal transport in fumarolic gases. J. Volcan. Geotherm. Res., 400: 106929.

Renggli, C.J., Hellmann, J.L., Burckhardt, C., Klemme, S., Berndt, J., Pangritz, P., Kleine, T., 2022. Tellurium evaporation from silicate melts and stable isotope fractionation, Geochim. Cosmochim. Acta, in press

Richter, F.M., Dauphas, N., Teng, F.Z., 2009. Non-traditional fractionation of non-traditional isotopes: Evaporation, chemical diffusion and Soret diffusion. Chem. Geol., 258(1-2): 92-103.

Richter, F.M., Janney, P.E., Mendybaev, R.A., Davis, A.M., Wadhwa, M., 2007. Elemental and isotopic fractionation of Type BCAI-like liquids by evaporation. Geochim. Cosmochim. Acta, 71(22): 5544-5564.

Richter, F.M., Mendybaev, R.A., Christensen, J.N., Ebel, D., Gaffney, A., 2011. Laboratory experiments bearing on the origin and evolution of olivine-rich chondrules. Meteor. Planet. Sci., 46(8): 1152-1178.

Roeder, P.L., Reynolds, I., 1991. Crystallization of chromite and chromium solubility in basaltic melts. J. Petrol., 32(5): 909-934.

Rubin, K., 1997. Degassing of metals and metalloids from erupting seamount and mid-ocean ridge volcanoes: Observations and predictions. Geochim. Cosmochim. Acta, 61(17): 3525-3542.

Rudge, J.F., Reynolds, B.C., Bourdon, B., 2009. The double spike toolbox. Chem. Geol., 265(3-4): 420-431.

Schoenberg, R. et al., 2016. The stable Cr isotopic compositions of chondrites and silicate planetary reservoirs. Geochim. Cosmochim. Acta, 183: 14-30.

Shen, J. et al., 2020. Stable chromium isotope fractionation during magmatic differentiation: Insights from Hawaiian basalts and implications for planetary redox conditions. Geochim. Cosmochim. Acta, 278: 289-304.

Sossi, P.A. et al., 2016. Petrogenesis and geochemistry of Archean komatiites. J. Petrol., 57(1): 147-184.

Sossi, P.A., Fegley, B., 2018. Thermodynamics of Element Volatility and its Application to Planetary Processes. In: King, P., Fegley, B., Seward, T. (Eds.), High Temperature Gas-Solid Reactions in Earth and Planetary Processes. Reviews in Mineralogy & Geochemistry, pp. 393-459.

Sossi, P.A., Klemme, S., O'Neill, H.S.C., Berndt, J., Moynier, F., 2019. Evaporation of moderately volatile elements from silicate melts: experiments and theory. Geochim. Cosmochim. Acta, 260: 204-231.

Sossi, P.A. et al., 2020. An experimentally-determined general formalism for evaporation and isotope fractionation of Cu and Zn from silicate melts between 1300 and 1500 degrees C and 1 bar. Geochim. Cosmochim. Acta, 288: 316-340.

Sossi, P.A., Moynier, F., van Zuilen, K., 2018. Volatile loss following cooling and accretion of the Moon revealed by chromium isotopes. Proc. Nat. Acad. Sci., 115(43): 10920-10925.

Stefansson, A. et al., 2017. Major impact of volcanic gases on the chemical composition of precipitation in Iceland during the 2014-2015 Holuhraun eruption. J. Geophys. Res. - Atmosph., 122(3): 1971-1982.

Trinquier, A., Birck, J.L., Allegre, C.J., 2008. High-precision analysis of chromium isotopes in terrestrial and meteorite samples by thermal ionization mass spectrometry. J. Analy. Atom. Spectr., 23(12): 1565-1574.
Tsuchiyama, A., Nagahara, H., Kushiro, I., 1981. Volatilization of sodium from silicate melt spheres and its application to the formation of chondrules. Geochim. Cosmochim. Acta, 45(8): 1357-1367.
Turgeon, S.C., Creaser, R.A., 2008. Cretaceous Anoxic Event 2 triggered by a massive magmatic episode. Nature, 454: 323–326.
Wagner, L.J. et al., 2021. Coupled stable chromium and iron isotopic fractionation tracing magmatic mineral crystallization in Archean komatiite-tholeiite suites. Chem. Geol., 576.
Wahrenberger, C., Seward, T.M., Dietrich, V., 2002. Volatile trace-element transport in high-temperature gases from Kudriavy volcano (Iturup, Kurile Islands, Russia), Water-Rock Interactions, Ore Deposits, and Environmental Geochemistry: A Tribute to David A. Crerar, pp. 307-327.
Wang, K., Jacobsen, S.B., 2016. Potassium isotopic evidence for the origin of the Moon. Nature, 538: 487-490.
Wijbrans, C.H., Klemme, S., Berndt, J., Vollmer, C., 2015. Experimental determination of trace element partition coefficients between spinel and silicate melt: the influence of chemical composition and oxygen fugacity. Contrib. Mineral. Petrol., 169: 45-77.
Wimpenny, J. et al., 2019. Experimental determination of Zn isotope fractionation during evaporative loss at extreme temperatures. Geochim. Cosmochim. Acta, 259: 391-411.
Yamakawa, A., Yamashita, K., Makishima, A., Nakamura, E., 2009. Chemical Separation and Mass Spectrometry of Cr, Fe, Ni, Zn, and Cu in Terrestrial and Extraterrestrial Materials Using Thermal Ionization Mass Spectrometry. Analytical Chemistry, 81(23): 9787-9794.
Yobo, L.N. et al., 2022. LIP volcanism (not anoxia) tracked by Cr isotopes during Ocean Anoxic Event 2 in the proto-North Atlantic region. Geochim. Cosmochim. Acta, 332: 138-155.
Yu, Y., Hewins, R.H., Alexander, C.M.O.D., Wang, J., 2003. Experimental study of evaporation and isotopic mass fractionationof potassium in silicate melts. Geochim. Cosmochim. Acta, 67: 773–786.
Zelenski, M., Simakin, A., Taran, Y., Kamenetsky, V.S., Malik, N., 2021. Partitioning of elements between high-temperature, low-density aqueous fluid and silicate melt as derived from volcanic gas geochemistry. Geochim. Cosmochim. Acta, 295: 112-134.
Zhu, J.-M., Wu, G., Wang, X., Han, G., Zhang, L., 2018. An improved method of Cr purification for high precision measurement of Cr isotopes by double spike MC-ICP-MS. J. Analy. Atom. Spectr., 33: 809–821.
Ziberna, L., Klemme, S., 2016. Application of thermodynamic modelling to natural mantle xenoliths: Examples of density variations and pressure-temperature evolution of the lithospheric mantle. Contrib. Mineral. Petrol., 171: 1-14.